Room Temperature Electrochemical Redox Reactions of the Defect Perovskite $SrFeO_{2.5+x}$

A. Nemudry,[†] M. Weiss,[‡] I. Gainutdinov,[†] V. Boldyrev,[†] and R. Schöllhorn*[,‡]

Institute of Solid State Chemistry, Siberian Branch, Russian Academy of Science, 630128 Novosibirsk, Russia, and Institut für Anorganische und Analytische Chemie, Technische Universität Berlin, 10623 Berlin, Germany

Received February 17, 1998. Revised Manuscript Received May 29, 1998

The electrochemical and chemical oxidation of the defect perovskite $SrFeO_{2.5}$ to the cubic perovskite $SrFeO_3$ at ambient temperature in alkaline electrolyte are shown to be in principle reversible processes with the appearance of intermediate compounds; the oxidation can be described by the formation of line phases $SrFeO_{2.75}$ and $SrFeO_{2.87}$ and one solid solution range $SrFeO_{3-x}$ with $0 \leq x \leq 0.03$. The structure of the brownmillerite type parent phase is characterized by the presence of stacking faults in the octahedral and tetrahedral sequence of layers whose concentration increases significantly upon formation of the intermediate phases. Models based on observed microscopic features are discussed in order to explain the unusual phenomenon of room temperature oxygen transport.

Introduction

Perovskite type oxides exhibiting ionic or mixed electronic/ionic conductivity are of considerable interest for potential application, e.g. as high-temperature solid oxide fuel cells, battery electrodes and sensor materials,[1,2] membranes for oxygen separation from air, and catalysts for the conversion of hydrocarbons.[3−6] One of the most essential features of these compounds is high oxygen mobility which—as has been shown in a large number of studies—drops at 600−800 °C, however, to a level that is no longer useful for practical purposes. Thus the development of oxygen ionic conductors that retain higher oxygen mobility at lower operating temperatures is of substantial interest.

Under these aspects it is most remarkable that in recent publications it has been reported that K_2NiF_4 type[7,8] and perovskite type[9,10] transition metal oxides are able to undergo topotactic oxygen uptake in the course of electrochemical reactions at *ambient temperature.*

The aim of the present work is the investigation of the reaction mechanism of electrochemical/chemical oxidation reactions of $SrFeO_{2.5}$ crystallizing in the brownmillerite type structure in order to define essential factors which are responsible for the unusual high reactivity of strontium oxoferrates at low temperatures.

Experimental Section

$SrFeO_{2.5}$ was prepared by standard solid-state techniques. Stoichiometric amounts of $SrCO_3$ and Fe_2O_3 (analytical grade) were ground and calcined in air at 900 °C for 12 h. The samples were pelletized and heated in air at temperatures of 1250 (24 h) and 1000 °C (12 h) and quenched thereafter in liquid N_2. To remove the rest of the oxygen excess, the pellets of $SrFeO_{2.5+x}$ were placed into a quartz ampule heated at 1000 °C under dynamic vacuum (10^{-2} Torr) for 6 h and quenched under vacuum in liquid N_2. Powder X-ray diffraction data were measured with a Siemens D 5000 diffractometer using Cu Kα radiation. X-ray diffraction and EDX measurements showed the absence of impurity phases in the parent compound. According to iodometric titration the samples had an oxygen stoichiometry corresponding to $SrFeO_{2.49(1)}$. Electrochemical experiments were performed at room temperature in galvanostatic mode (three electrode cell, 1 N KOH electrolyte) with working electrodes of polycrystalline material: (i) prepared as sintered pellets; (ii) pressed into Pt grids along with 1 wt % of Teflon and 15−20 wt % acetylene black. In situ X-ray diffraction measurements were carried out in specially designed three electrode cells with Hg/HgO as the reference electrode and the working electrode as the diffraction object. Nominal current densities in galvanostatic experiments are given in terms of current per mass unit of working electrode material and varied between 0.02 and 3 μA/mg. Chemical oxidation reactions were carried out with powdered samples in aqueous suspension with alkaline sodium hypobromite at 0 °C. Chemical reduction was performed in 60% aqueous hydrazine hydrate. For chemical analysis EDX and iodometric titration were used.

The Mössbauer spectroscopy measurements were carried out by conventional constant acceleration technique at room

* Corresponding author.
[†] Russian Academy of Science.
[‡] Technische Universität Berlin.

(1) Steele, B. C. H. *Mater. Sci. Eng.* **1992**, *B13*, 79.
(2) Tu, H. Y.; Takeda, Y.; Imanishi, N.; Yamamoto, O. *Solid State Ionics* **1997**, *100*, 283.
(3) Qiu, L.; Lee, T. H.; Liu, L.-M.; Yang, Y. L.; Jacobson, A. J. *Solid State Ionics* **1995**, *76*, 321.
(4) Chen, C. H.; Bouwmeester, H. J. M.; van Doorn, R. H. E.; Kruidhof, H.; Burggraaf, A. J. *Solid State Ionics* **1997**, *98*, 7.
(5) Pei, S.; Kleefisch, M. S.; Kobylinski, T. P.; Faber, J.; Udovich, C. A.; Zhang-McCoy, V.; Dabrowski, B.; Balachandran, U.; Mieville, R. L.; Poeppel, R. B. *Catal. Lett.* **1995**, *30*, 201.
(6) Schinzer, C.; Saymeh, R. A.; Asfour, H. M. *Z. Naturforsch.* **1997**, *52B*, 927.
(7) Wattiaux, A.; Park, J. C.; Grenier, J.-C.; Pouchard, M. *C. R. Acad. Sci.* **1990**, *310* (II), 1047.
(8) Rudolf, P.; Paulus, W.; Schöllhorn, R. *Adv. Mater.* **1991**, *3*, 438.
(9) Wattiaux, A.; Fournés, L.; Demourgues, A.; Bernaben, N.; Grenier, J.-C.; Pouchard, M. *Solid State Commun.* **1991**, *77*, 489.
(10) Nemudry, A.; Rudolf, P.; Schöllhorn, R. *Chem. Mater.* **1996**, *8*, 2232.

S0897-4756(98)00090-8 CCC: $15.00
Published on Web 08/13/1998

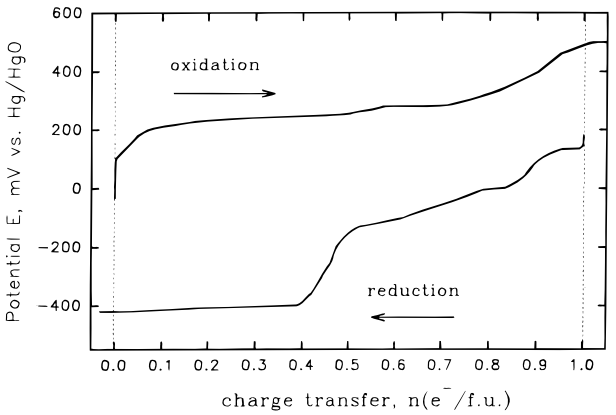

Figure 1. Galvanostatic anodic oxidation and subsequent cathodic reduction of the brownmillerite type defect perovskite $SrFeO_{2.5}$ at 300 K in 1 M aqueous KOH electrolyte: change of potential E with charge-transfer n; the correlation between the oxygen stoichiometry index x and the charge-transfer value n is $x = n/2$.

Table 1. Structural Data for Strontium Ferrates

	unit cell params (Å)				
compd	a	b	c	$a^*_{calc} = [abc]^{1/3}$ [b]	a^*_{expt} [a]
$SrFeO_{2.5}$[a]	5.668(1)	15.576(1)	5.530(1)	3.938	
$SrFeO_{2.73}$[b]	10.972(6)	7.700(5)	5.471(3)	3.866	3.866(1)
$SrFeO_{2.86}$[b]	10.934(6)		7.705(5)	3.861	3.861(1)
$SrFeO_{2.97}$[b]	3.855(3)			3.855	
$SrFeO_{3.0}$[a]	3.850(1)			3.850	

[a] Electrochemical data, this work. [b] Data for thermal phases according to ref 11.

temperature. The isomer shift data were given relative to the isomer shift of α-iron.

Electron diffraction and microscopy studies have been performed on a JEM-2000FX at an accelerating power of 200 kV.

Results and Discussion

The variation of the potential of the working electrode material $SrFeO_{2.5+x}$ with the charge transfer obtained in galvanostatic mode at a current density of 1 μA/mg during the oxidation and reduction processes given in Figure 1. After a charge transfer of $n = 1$ e$^-$/$SrFeO_{2.5}$ that corresponds to the formation of $SrFeO_{3.0}$ oxygen evolution is observed; lattice parameters and analytical composition (Table 1) remain constant on continued oxidation. Maximal charge transfer at $n = 1$ e$^-$/$SrFeO_{2.5}$ is confirmed by iodometric titration and Mössbauer spectroscopy measurements (Table 1).

As is expected, the galvanostatic reaction is strongly influenced by kinetics. High current densities > 1.5 μA/mg result in strong overpotentials, particularly in the initial section of the oxidation, oxygen evolution starts below a nominal charge transfer of $n = 1$ e$^-$/fu, and no quantitative reaction is observed at $n = 1$, i.e., the value calculated from eq 1. Clear end points with quantitative conversion corresponding to eq 1 at $n = 1$ e$^-$/fu could be obtained at low current densities of 1 μA/mg.

$$SrFeO_{2.5} + {}^1/_2O^{2-} \rightarrow SrFeO_{3.0} + 1e^- \qquad (1)$$

For the cathodic galvanostatic reduction (eq 2) no pronounced end point is found in the potential/charge-transfer curve (Figure 1). Hydrogen evolution is observed, however, with current densities of ≈1 μA/mg at $n = 1$ e$^-$/fu; quantitative reduction was obtained only for pressed working electrodes with an addition of 20% acetylene black. This is a consequence of the low electronic conductivity of the terminal phase $SrFeO_{2.5}$. The X-ray patterns of reduced samples are characterized by rather broad reflections. At extended reaction times additional reflections indicate the formation of $SrCO_3$, which is evidence for a slow partial degradation of strontium oxoferrate in aqueous medium. Structural data for the starting $SrFeO_{2.5}$ and the product of electrochemical oxidation are given in Table 1.

$$SrFeO_3 + H^+ + e^- \rightarrow SrFeO_{2.5} + {}^1/_2H_2O \qquad (2)$$

The *chemical* oxidation of $SrFeO_{2.5}$ according to eq 1 was achieved by treatment with excess aqueous sodium hypobromite in suspension at 0 °C. Under these conditions it was possible to obtain a cubic product as determined by X-ray diffractometry; from the lattice parameters a stoichiometry of $SrFeO_{2.9}$ was calculated. If the reaction is carried out at ambient temperature, partial irreversible decomposition of the material is observed.

The chemical reduction according to eq 2 was performed with hydrazine hydrate at room temperature; it is accompanied by partial degradation of the oxoferrate phase and significant X-ray line broadening. It is obvious that the electrochemical reactions proceed much more reliably as compared to the chemical reactions under the conditions applied.

In Situ X-ray Diffraction Studies. The specific shape of the potential/charge-transfer curves obtained in the electrochemical redox reaction (Figure 1) suggests the presence of intermediate phases between educt and terminal product. For a more detailed investigation of the reaction mechanism we therefore performed in situ X-ray diffraction studies under conditions similar to those described earlier.[10] Figure 2 displays sections of characteristic diffractograms obtained in the course of the oxidation of $SrFeO_{2.5}$.

It is useful at this point to take into consideration the phases identified in the $SrFeO_z$ system upon *thermal* preparation (related to the cubic perovskite cell):[11] brownmillerite structure (index b, $z = 2.5$) with $a_b \approx 2a_c$, $b_b \approx 4a_c$, $c_b \approx 2a_c$; orthorhombic phase (index o, $2.68 < z < 2.73$) with $a_o \approx 2\sqrt{2}a_c$, $b_o \approx 2a_c$, $c_o \approx \sqrt{2}a_c$; tetragonal line phase (index t, $z = 2.87$) with $a_t = b_t \approx 2\sqrt{2}a_c$, $c_t \approx 2a_c$; cubic perovskite (index c, $2.97 < z < 3.0$) (Table 1).

Orthorhombic and tetragonal distortions related to the specific ordering of the oxygen vacancies are rather small and have been detected only by the use of Cu Kβ radiation. The existence of the phases mentioned above has been confirmed by Mössbauer spectroscopy as discussed below.[11]

In the case of in situ X-ray diffraction measurements of the electrochemical oxidation of $SrFeO_{2.5}$ at room temperature the structural studies are complicated by broadening of the reflections, which is likely to be due to the formation of structural defects which cannot be annealed at ambient temperature. The oxidation was

(11) Takeda, Y.; Kanno, K.; Takado, T.; Yamamoto, O.; Takano, M.; Nakayama, N.; Bando, Y. *J. Solid State Chem.* **1986**, *63*, 237.

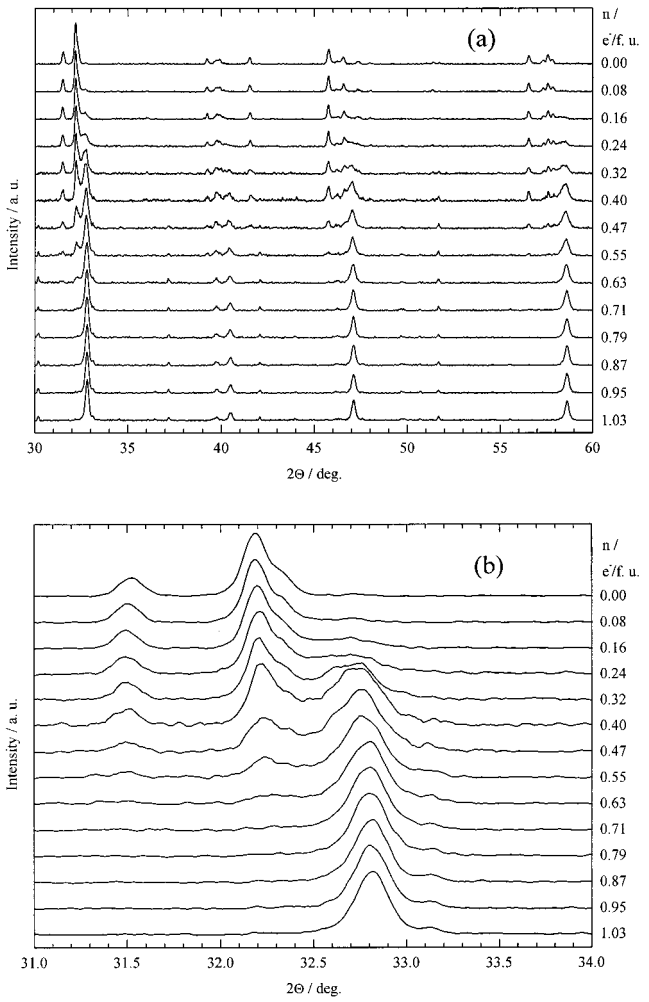

Figure 2. In situ measurement of the anodic oxidation of $SrFeO_{2.5}$: (a) X-ray patterns for selected charge-transfer values; (b) enlarged section showing the transition for the strongest reflection.

found to proceed with the formation of intermediate phases that can be indexed with pseudocubic symmetry (Figures 2 and 3). In a first simple approach the data can be described by two regions: (i) $0 < n < 0.5$ as two phase range and (ii) $0.5 < n < 1.0$ as one phase range. A more thorough analysis of the changes in electrode potential and line widths of the Bragg reflections with the charge transfer leads to a division into three different sections.

The first range I with $0 < n < 0.5$ and approximately constant potential is characterized by the coexistence of the educt phase $SrFeO_{2.5}$ and a new phase $SrFeO_{2.75}$ with broad and asymmetric reflections. The lattice parameter ($a^*_{expt} = 3.866(1)$ Å), which was evaluated in cubic approximation, is similar to the reduced averaged parameter for thermally prepared $SrFeO_{2.75}$ ($a^*_{calc} = [a_o b_o c_o]^{1/3}/8 = 3.866$ Å) (Table 1). The high value of the line width full width at half-maximum (fwhm) and the asymmetry of the X-ray reflections of the intermediate compound in this range is in agreement with orthorhombic splitting for the $SrFeO_{2.75}$ lattice, which cannot be resolved, however, because of the imperfection of the crystal lattice of the intermediate and lower resolution of the Cu Kα radiation which has been used.

The second range II ($0.5 < n < 0.75$) is characterized by a plateau in the potential/charge transfer diagram,

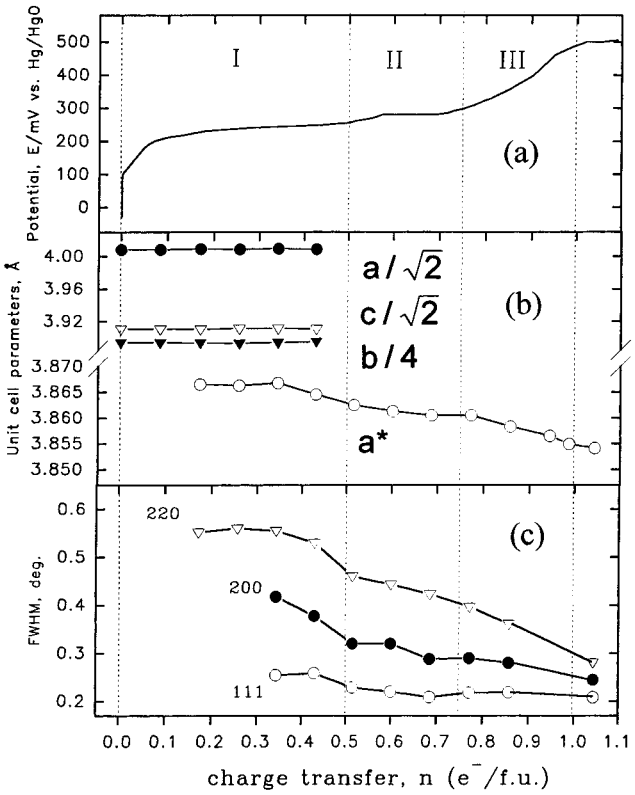

Figure 3. In situ anodic oxidation of $SrFeO_{2.5}$: (a) potential E vs charge-transfer n; (b) change of unit cell parameters with n; (c) variation of line width of selected reflections ("cubic phase") vs charge transfer n.

an almost constant unit cell parameter, and a decrease in the line width. It can be assigned to a two phase region with the coexistence of $SrFeO_{2.75}$ and $SrFeO_{2.87}$. The pseudocubic parameter ($a^*_{expt} = 3.861(1)$ Å) of the latter is in agreement with the averaged reduced parameter ($a^*_{calc} = [a_t b_t c_t]^{1/3}/16 = 3.861$ Å) for thermally prepared $SrFeO_{2.86}$ phases (Table 1). The drop of the line width correlates with the disappearance of orthorhombic and formation of a tetragonal distortion which is smaller. The transition region with the coexistence of $SrFeO_{2.75}$ and $SrFeO_{2.87}$ in this experiment cannot be resolved because of the proximity and broadening of the reflections which simulates a continuous shift of averaged lattice parameters.

The third range III ($0.75 < n < 1.0$) which is characterized by continuous changes in potential, lattice parameters, and line width can be interpreted as a one phase reaction with a transformation of the tetragonal structure $SrFeO_{2.87}$ to the cubic perovskite $SrFeO_{3.0}$.

Figures 4 and 5 present selected regions of diffractograms and data of in situ X-ray diffraction measurements of the electrochemical *reduction* of $SrFeO_{3.0}$ at room temperature. The reduction proceeds almost symmetrically in terms of the formation of pseudocubic intermediates and changes in their lattice parameters and line widths. Again the process can be divided into three ranges.

The first range I* ($0 < n < 0.25$) can be interpreted as continuous transformation of the cubic perovskite $SrFeO_{3.0}$ to the tetragonal $SrFeO_{2.87}$. It is characterized by a considerable increase of the width of reflections toward the end of this range which is due to the formation of a tetragonal distortion in the lattice (Figure

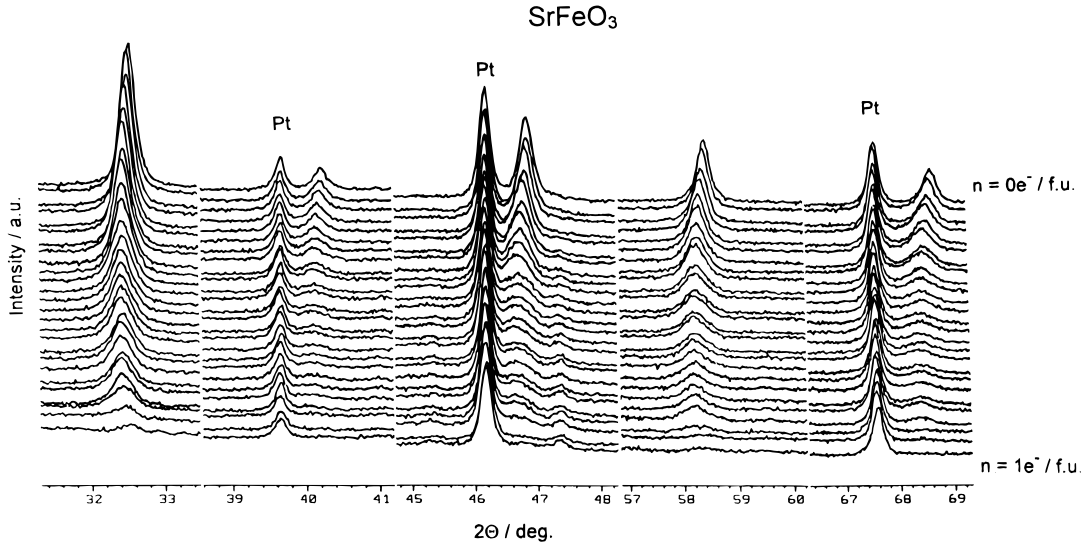

Figure 4. In situ cathodic reduction of $SrFeO_3$: sections of diffractograms with different charge transfer n: (top) $SrFeO_3$ ($n = 0$); (bottom) terminal phase $SrFeO_{2.5}$ ($n = 1$); (intervals) 0.04 e^-/fu.

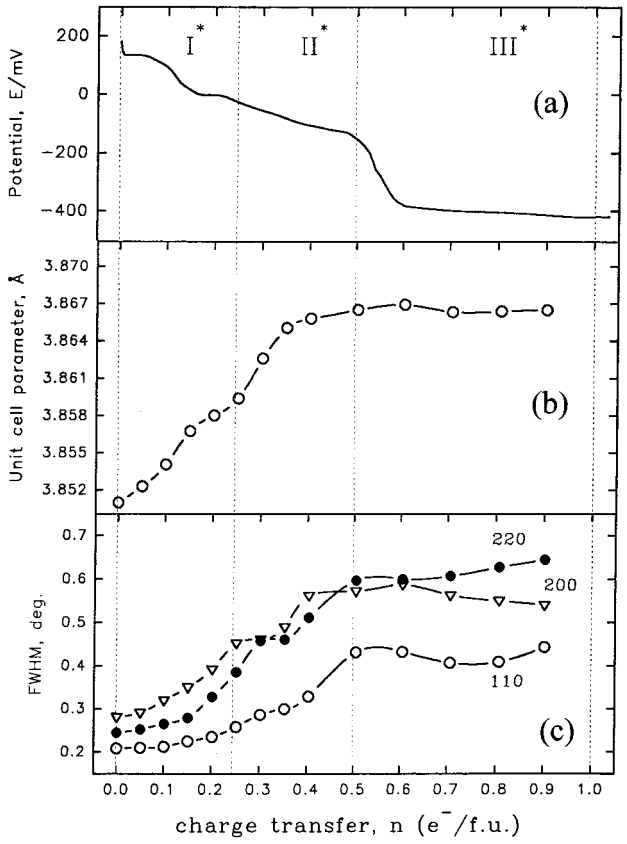

Figure 5. In situ reduction of $SrFeO_{3.0}$: potential E; lattice parameters and variation of line width of reflections ("cubic phase") vs charge transfer n.

5c). In the range of $0.06 < n < 0.25$ of the potential/charge-transfer diagram there is a small plateau which is kinetically distorted toward the border region. Similar to observations with phases obtained by thermal preparation,[11] this can be related to the existence of a two phase region between the lower limit of $SrFeO_{3-x}$ ($0 \leq x \leq 0.03$) and the line phase $SrFeO_{2.87}$.

The second range II* ($0.25 < n < 0.5$) which is characterized by the presence of a distorted plateau, of a further increase of the line width, and of the a axis length can be interpreted as a two phase region with the formation of $SrFeO_{2.75}$. The increase of the line width up to the highest values corresponds with the appearance of orthorhombic splitting of the reflections (Figure 5). In this region the pseudocubic parameter varies between 3.859(1) and 3.865(1) Å, which is close to pseudocubic parameters obtained in the course of electrochemical oxidation of $SrFeO_{2.5}$ and averaged reduced parameters of thermally prepared phases $SrFeO_{2.87}$ and $SrFeO_{2.75}$, respectively (Table 1).

The third range III* ($0.5 < n < 1.0$), which is characterized by a potential plateau of the galvanostatic curve and a decrease of the line intensity at almost constant pseudocubic parameter, can be described as a two phase reaction with the formation of brownmillerite with broad reflections.

The X-ray diffraction analysis of the electrochemical redox cycle carried out via in situ mode shows the principal reversibility of the process. Intermediate phases $SrFeO_{2.75}$, $SrFeO_{2.87}$, and $SrFeO_{3-x}$ ($0 \leq x \leq 0.03$), which have a structural relationship based on the perovskite lattice, reveal a high degree of imperfection that leads to considerable broadening of reflections. The electrochemical reduction turned out to be strongly dependent upon the electrode material. Reduction to $SrFeO_{2.5}$ could only be achieved with specially prepared pressed powder electrodes (cf. above); the additions required lead, however, to a decrease in the quality of the X-ray diagrams and accelerated partial decomposition. In contrast, upon the use of sintered pellet electrodes no decomposition is observed; the reversibility in cycling tests is excellent but is limited to a lower stoichiometry of $SrFeO_{2.8}$ presumably due to the strong decrease in electronic conductivity with the decreasing average oxidation state of iron. Similar problems were not observed for the related oxocobaltate system $SrCoO_{2.5+x}$,[10] which exhibits good electronic conductivity in the whole redox range as well as superior chemical stability in aqueous electrolytes. Since the investigation of the reduction process is complicated by the reasons discussed above, Mössbauer and electron microscopy studies have been limited to the oxidation process.

Ex Situ Mössbauer Spectroscopy Studies of the Electrochemical Oxidation. To support the phase

diagram discussed above, we have used Mössbauer spectroscopy studies which can provide local information and do not depend on the crystal perfection as X-ray diffraction. The initial measurements were performed both with products derived from electrochemical oxidation with sintered electrodes and with pressed powder electrodes. As discussed below in more detail it turned out that data from materials obtained via pressed powder electrodes could not be used due to partial decomposition. The Mössbauer and electron microscopy data were restricted therefore to products prepared from sintered pellet electrodes.

Thermally prepared phases $SrFeO_z$ ($2.5 < z < 3.0$) have been intensively studied earlier by Mössbauer spectroscopy.[12−17] It was found that compounds with $z = 2.5$, 2.75, 2.86, and 3.0 exhibit characteristic spectra due to specific vacancy ordering. The phase analysis performed in the following is based on the presence of characteristic Mössbauer spectra for each phase. For the brownmillerite phase there are two characteristic sextets: the $SrFeO_{2.75}$ phase exhibits a doublet with a quadrupole splitting $\Delta E = 1$ mm/s and an isomer shift of 0.3 mm/s; the $SrFeO_{2.86}$ phase shows the $Fe^{3.5+}$ doublet with $\Delta E = 0.56$ and 0.17 mm/s.[12−17] The strong relationship in the intensity of components of each phase provides the possibility of estimating the total phase content in the electrochemically oxidized sample.

Mössbauer spectroscopy studies of samples oxidized galvanostatically as described above were carried out in ex situ mode. Directly after electrochemical treatment the pressed powder electrodes were washed by distilled water, dried in air, and placed in the Mössbauer spectrometer along with the platinum net. The sintered pellet electrodes after electrochemical treatment were ground to powder for Mössbauer studies. Results which we obtained for both types of samples turned out to be different.

According to the ex situ Mössbauer study the pressed powder electrode samples obtained after electrochemical oxidation are not stable and their extended contact with electrolyte or aqueous media results in partial degradation. This is confirmed by the appearance of the specific doublet X Fe^{3+} (=0.337 and $\Delta E = 0.66$ mm/s), which has been earlier assigned to a product of degradation of the $SrFeO_{2.89}$ after its contact with water or aqueous solution of KOH.[14]

The ex situ Mössbauer study of electrochemically oxidized sintered dense pellets reveals the absence of the doublet X even in the fully oxidized samples (Figure 6). Therefore we conclude that the process of the degradation of Fe^{4+} can be suppressed by the decrease of the surface area in contact with electrolyte. In Table 2 ex situ Mössbauer data for sintered pellets are summarized. The sample which was prepared by the passing of a charge that is equivalent $n = 0.32$ e^-/fu contains two splitted sextets of $SrFeO_{2.5}$ (49.5%) and

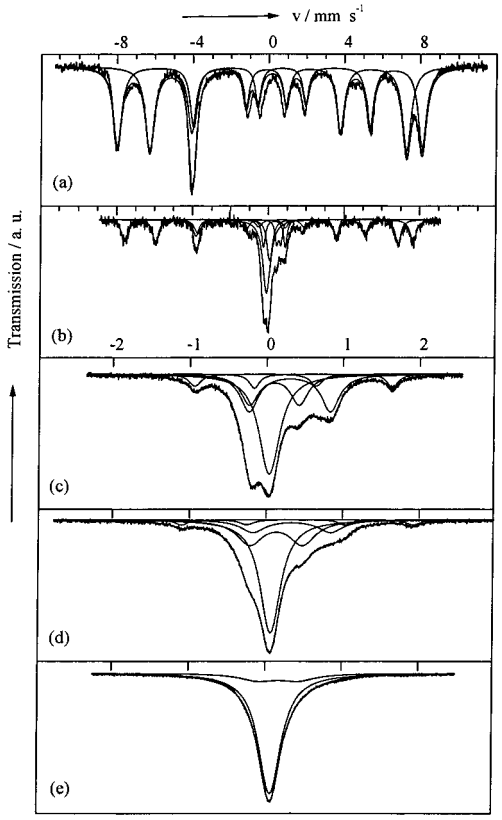

Figure 6. Mössbauer spectra obtained for oxidized sintered pellets with different charge transfer: (a) starting brownmillerite; (b and c) $n = 0.32$ e^-/fu; (d) 0.5 e^-/fu; (e) $n = 1.0$ e^-/fu.

Table 2. Mössbauer Data for Electrochemically Oxidized Sintered Pellets of $SrFeO_{2.5}$

charge transfer	N	δ, mm/s	ΔE, mm/s	H, mm/s	G, mm/s	%
	1	0.372	−0.325	15.24	0.476	25
	2	0.179	0.281	12.81	0.5	23
0.32	3	0.3	1.06		0.288	13
	4	0.1	0.649		0.278	13
	5	0.0326			0.367	26
	1	0.367	−0.312	16.15	0.373	10
	2	0.2	0.293	13.59	0.331	11
0.5	3	0.355	1.1		0.48	16
	4	0.132	0.709		0.297	20
	5	0.05			0.329	41
	1	0.31	1.085		0.25	5
0.75	2	0.175	0.57		0.4	31
	3	0.068			0.31	64
1.0	1	0.3	0.5		0.6	5
	2	0.05			0.3	95

characteristic components which belong to $SrFeO_{2.75}$ (30%) as expected for a two phase region; the signal characteristic for $SrFeO_{2.87}$ (20%) is present also, however (Figure 6b, Table 2). The sample with a charge transfer of $n = 0.5$ e^-/fu (Figure 6d) still contains an unreacted fraction of brownmillerite structure (21%). The volume fractions of orthorhombic $SrFeO_{2.75}$ and tetragonal $SrFeO_{2.87}$ increased up to 36 and 41%, respectively. Further oxidation leads to consecutive disappearance of the brownmillerite spectrum, diminishing components of $SrFeO_{2.75}$ and $SrFeO_{2.87}$ phases, and an increase of the singlet of $SrFeO_{3.0}$ (Table 2). The final product of the oxidation contains almost 100% iron ion with the oxidation state Fe^{4+} (Figure 6e).

Thus, despite inhomogeneous progress of the reaction in dense sintered pellets, ex situ Mössbauer data

(12) Fournés, L.; Potin, Y.; Grenier, J.-C.; Demazeau, G.; Pouchard, M. *Solid State Commun.* **1987**, *62*, 239.
(13) Gibb, T. C. *J. Mater. Chem.* **1994**, *4*, 1445.
(14) Fierra, C.; Carbonio, R. E.; Scherson, D.; Yeager, E. B. *Electrochim. Acta* **1988**, *33*, 941.
(15) Takano, M.; Okita, T.; Nakayama, N.; Bando, Y.; Takeda, Y.; Yamamoto, O.; Goodenough, J. B. *J. Solid State Chem.* **1988**, *73*, 140.
(16) Takano, M.; Takeda, Y. *Bull. Inst. Chem. Res., Kyoto Univ.* **1983**, *61*, 406.
(17) Gibb, T. C. *J. Chem. Soc., Dalton Trans.* **1985**, 1455.

correspond with data obtained by Takeda et al.[11] on thermal phases and confirm the formation of the orthorhombic $SrFeO_{2.75}$, tetragonal $SrFeO_{2.87}$, and cubic $SrFeO_{3-x}$ phases in the course of electrochemical oxidation at room temperature.

The Mössbauer data appear not to be in agreement with a pseudo one phase behavior of lattice parameters obtained in the course of in situ X-ray studies. Takeda et al.[11] have observed that $SrFeO_{2.88}$ samples had an almost cubic perovskite type structure according to X-ray data, in spite of the fact that Mössbauer spectra were close to those of the tetragonal phase. It was suggested that the sample consists of two types of microdomains having structures and compositions related to the cubic ($z \approx 3$) and tetragonal ($z \approx 2.87$) phases. These coherently packed domains have strong structural similarity but are highly disordered. It is an averaged structure close to cubic symmetry as observed by X-ray diffraction. The increase of the oxygen content in the samples is accompanied by an increase of the number and total volume of cubic domains to make the averaged unit cell volume smaller than observed experimentally. A similar situation has been also suggested for another intermediate region between orthorhombic and tetragonal phases. Therefore, pseudo one phase behavior of the lattice parameter and broadening of the reflections in the course of the electrochemical redox reaction can be related to the same phenomenon. For this reason we have studied the microstructure of electrochemically oxidized samples by electron microscopy.

Ex Situ Electron Microscopy Studies of the Electrochemical Oxidation. To avoid inhomogeneous progress of reaction, the samples of intermediate products for electron microscopic studies were prepared in quasi-equilibrium mode by using rather low currents ($I = 0.02\ \mu$A/mg) and sintered pellets of $SrFeO_{2.5}$ as the working electrode. The data of chemical analysis were in agreement with the calculated charge transfer.

Figure 7 represents electron diffraction patterns of samples with $n = 0$, 0.5 and 0.75 e^-/fu which clearly show the presence of $SrFeO_{2.75}$ and $SrFeO_{2.87}$ intermediate phases. All spots of these patterns have been indexed in agreement with structural data reported by Takeda et al.[11] (Table 1). The absence of diffraction patterns for the $SrFeO_3$ sample is related to its instability under the reducing conditions of the electron microscope; in the course of the exposition the diffraction picture changed due to progressing reduction of the compound.

The formation of orthorhombic $SrFeO_{2.75}$ and tetragonal $SrFeO_{2.87}$ intermediate phases in the course of the room temperature electrochemical oxidation is confirmed thus by electron diffraction.

It is important, however, to notice that starting material and intermediates have similar and quite specific diffraction patterns which are represented in Figure 8. The specific feature of these electron diffraction patterns which are visible for certain zone axis orientations of the samples is the presence of even rows of sharp spots which are periodically alternating with odd rows of the elongated spots streaking along the b^* direction for $SrFeO_z$ compounds with $z = 2.5$, 2.75 and the c^* direction for $z = 2.87$ (compare with Table 1). An

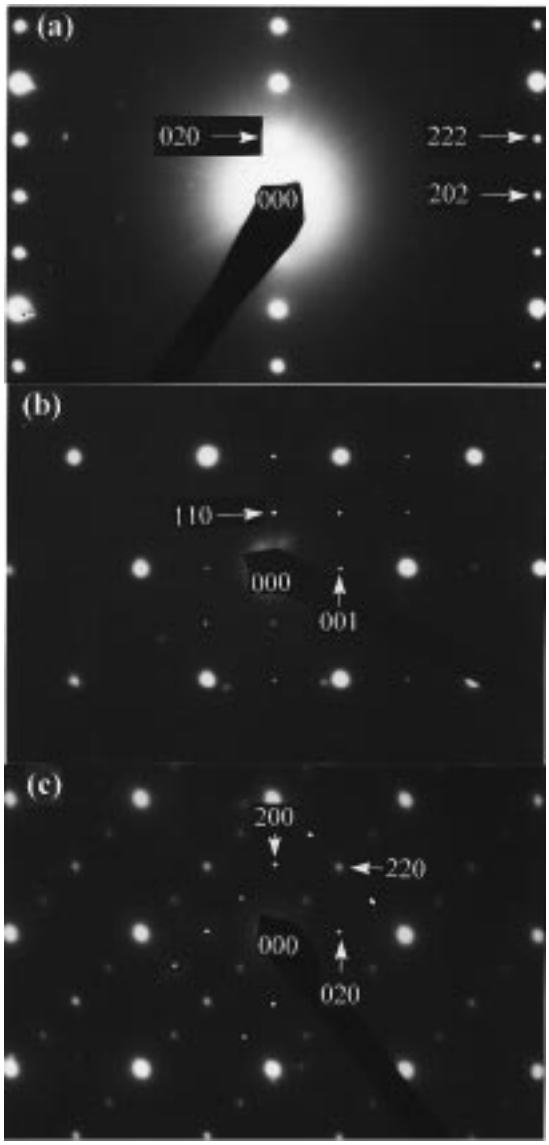

Figure 7. Electron diffraction patterns of (a) $SrFeO_{2.5}$ along the [10$\bar{1}$] zone axis; (b) $SrFeO_{2.75}$ along the [110] zone axis; (c) $SrFeO_{2.87}$ along the [001] zone axis.

attempt to index these patterns reveals that the spots of even rows belong to the phases $SrFeO_{2.5}$, $SrFeO_{2.75}$, and $SrFeO_{2.87}$. However, in this case elongated reflections of odd rows have the fraction values of hkl that can be related to the presence of superstructure cells with $2a \times 2b \times c$ lattice parameters for $z = 2.5$, 2.75 and $2a \times 2c$ for tetragonal $SrFeO_{2.87}$. Dark field image pictures (Figure 9) obtained by the use of elongated reflections show the alternation of dark and light stripes which are perpendicular to the b^* direction for $SrFeO_{2.5}$ and $SrFeO_{2.75}$ and to the c^* direction for $SrFeO_{2.87}$ (compare with Table 1).

The diffraction phenomena described above and microscopic images are well-known for compounds having polytype modifications.[18] These have been interpreted earlier as the formation of stacking faults by the translation of the layers relative to each other on (unit cell parameter)/2, e.g. $a/2$, which results in the disordering of the sequence of layers AAABBABA... and the

(18) *Electron microscopy in mineralogy*; Wenk, H.-R., Ed.; Springer-Verlag: Berlin, 1976.

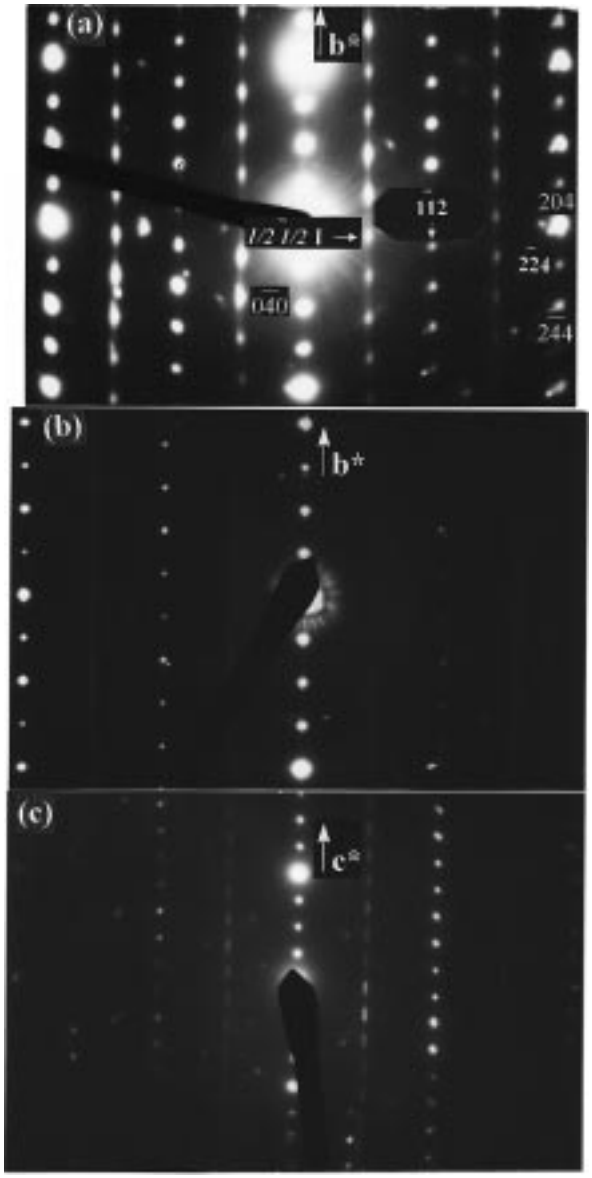

Figure 8. Electron diffraction patterns of (a) $SrFeO_{2.5}$ along the $[20\bar{1}]$ zone axis; (b) $SrFeO_{2.75}$ and (c) $SrFeO_{2.87}$ along the corresponding zone axes.

appearance of diffuse streaks with $h = 2n + 1$ oriented along, e.g., the b^* direction and sharp spots with $h = 2n$. Stacking faults are well-observed in the dark field image as a sequence of dark and light stripes. The intermediate state with a partially ordered sequence of stacking faults is characterized by the overlapping of diffuse streaks with sharp superstructure reflections that represent elongated spots.

The diffraction pattern for $SrFeO_{2.5}$ can be interpreted in the following way. It is known that the brownmillerite structure based on the perovskite lattice can be represented as a sequence of octahedral (O) and tetrahedral (T) layers OTOT′OTOT′... along the b axis.[19] In principle there is the probability of a defect formation in the sequence of octahedral and tetrahedral layers of brownmillerite which are similar to stacking faults taking into account that the sample was quenched to liquid N_2. In the case of a preservation of the overall

(19) Grenier, J.-C.; Ea, N.; Pouchard, M.; Hagenmüller, P. *J. Solid State Chem.* **1985**, *58*, 243.

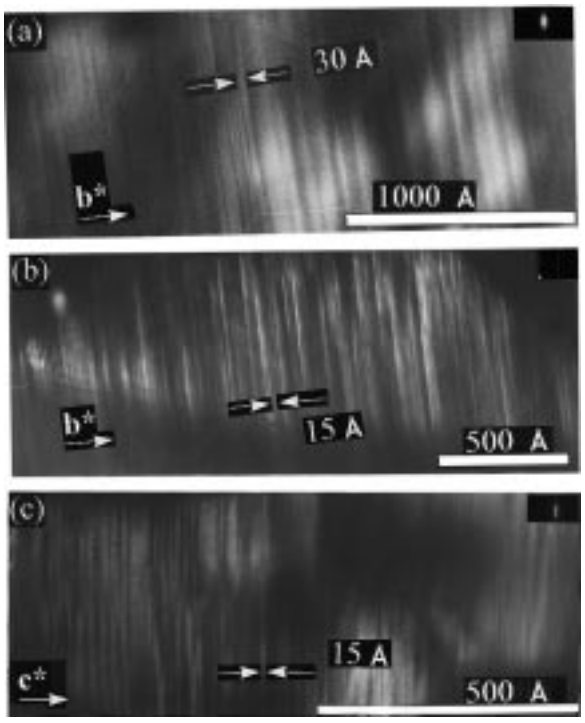

Figure 9. Dark field images of (a) $SrFeO_{2.5}$; (b) $SrFeO_{2.75}$ and (c) $SrFeO_{2.87}$ obtained by the use of the elongated spots.

composition for $SrFeO_{2.5}$, two main types of stacking defects are possible which are shown in Figure 10. These periodic stacking faults result in the formation of a superlattice with doubled b_b parameter. In the case of defect type I this is equivalent to a translation of the tetrahedral layers on $a_b/2$ toward each other (Figure 10). This almost periodic distribution of stacking defects in the brownmillerite lattice is in agreement with the observed diffraction phenomena for $SrFeO_{2.5}$ and dark field images. Moreover, on the microscopic pictures there are regions where the stripes alternate with a periodicity of ca. 30 Å that corresponds to a doubled b_b parameter of $SrFeO_{2.5}$ (compare with Table 1).

Diffraction patterns for $SrFeO_{2.75}$ and $SrFeO_{2.87}$ (Figure 8b,c) obtained along the corresponding zone axis are quite similar to the pattern of $SrFeO_{2.5}$ described above and can be interpreted in the same way. We have to stress that the degree of disorder in the OT... layer sequence is highest for $SrFeO_{2.75}$; the elongated along b^* direction spots were completely transformed to streaks (Figure 8b). The dark field image for $SrFeO_{2.75}$ corresponds with this; on the microscope images one can see a periodic sequence of stripes having 15 Å in width (Figure 9b) which reflects a doubled b_o lattice parameter for $SrFeO_{2.75}$ (compare with Table 1). For $SrFeO_{2.87}$ again there are odd elongated spots on the electron diffraction patterns and stripes 15 Å in width on dark field images which reflect the existence of ordered stacking faults forming a superstructure with doubled c_t lattice parameter (compare with Table 1).

We assume that the increase of disorder in $SrFeO_{2.75}$ is related to the oxygen intercalation, because oxygen uptake increases the probability of the interruption of the OTOT... layer sequence. The increase of stacking disorder results in both the formation of a pseudosymmetry and the broadening of the X-ray diffraction reflections as it has been detected in the course of in

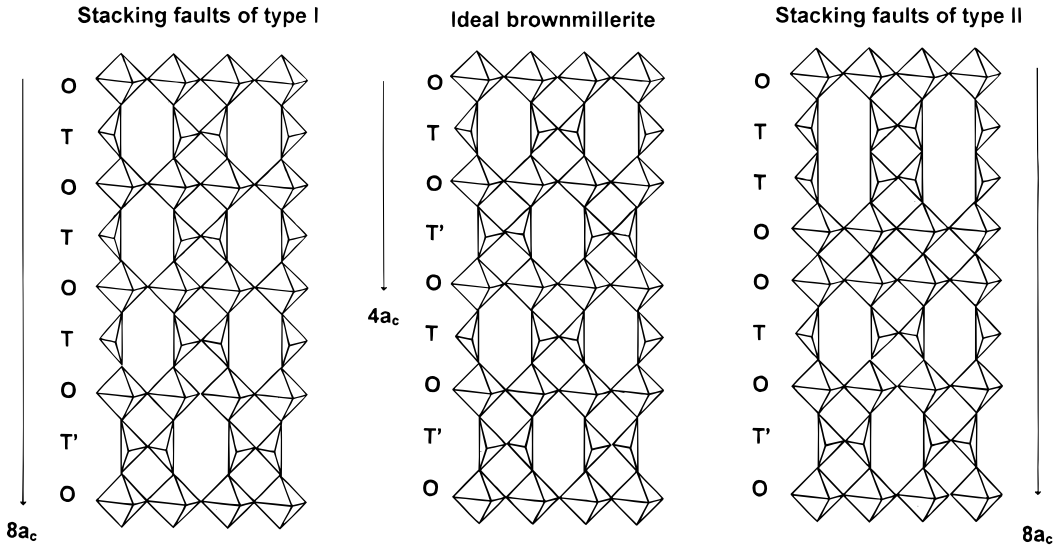

Figure 10. Scheme of the brownmillerite structure and of two possible polytype modifications appearing as stacking faults in the course of the reaction.

situ X-ray studies. The intercalation process increases moreover the probability of the formation of OO... perovskite-like motives. In this case disorder in the stacking sequence might be considered as structural intergrowth, i.e., coherent packing of perovskite-related microdomains with different oxygen stoichiometry. An increase of their volume fraction might be responsible for the seemingly continuous change of the averaged structural parameter as it was observed by the in situ X-ray diffraction studies.

Models for Low-Temperature Oxygen Mobility. The observation of a strong increase in concentration of defects in the course of the electrochemical oxygen intercalation at room temperature by electron microscopy leads us back to the problem of the unusual low-temperature oxygen transport in perovskite-related structures on another level. As we have already discussed earlier,[10] the high reactivity of these solids in the course of intercalation may depend either on a high intrinsic mobility of the guest species or on a high concentration of specific structural defects which are present or can arise in the course of the reaction.

A potential model for high intrinsic mobility of oxygen anions has been suggested earlier[10,20,21] on the basis of the presence of monovalent O^- species with reduced charge/radius ratio originating from the unusual high valence state of the transition metal ion (Fe^{4+}). There is no direct evidence so far, however, that a transport mechanism of this kind is involved in the room temperature oxidation process discussed here.

It is known that some brownmillerite type compounds are oxygen ionic conductors at 800−900 °C.[22−26] It has been observed that the operating temperature of these phases is drastically reduced to lower temperatures (≈400 °C) for intergrowth structures brownmillerite/perovskite (e.g. $Ba_3In_2MO_8$) with a sequence of octahedral and tetrahedral layers.[22] The model proposed to explain the increased ionic conductivity is based on a reduction of the activation energy for site change by the spatial separation of carriers (interstitials or vacancies) from Coulomb traps M^{4+} by location in different layers which results in enhanced charge screening.

In the present case of oxygen intercalation the insertion of guest ions can be described at low guest concentrations as the formation of interstitial type defects. If the trapping centers (Fe^{4+}) and carriers are located in different layers, then a charge screening similar to the one discussed above can be assumed. At higher oxygen stoichiometries we have to take into account, however, the association and local ordering of these point defects which renders the situation more complex.

A further model to be discussed here is related to the well-known fact that the high reactivity of solids in topotactic reactions can be a consequence of the presence of *specific extended defects* which exist or can arise in the course of reaction.[27,28] For instance, dislocations, domain, and antiphase boundaries can be potential channels with low activation energy for oxygen diffusion. The coefficient of diffusion along these defects can be 6−8 orders of magnitude higher as compared to the bulk of the material.

From this point of view the unusual high reactivity of the $SrFeO_{2.5}$ can also be explained in the following way. According to the data obtained in this work $SrFeO_{2.5}$ contains biographical extended defects as stacking faults. These can be considered as domain and antiphase boundaries which separate either regular brownmillerite domains from each other (type I; see text above, Figure 10) or OO...-perovskite-like and brownmillerite slabs from each other (type II; see text above, Figure 10). Stacking faults of type II can be assumed

(20) Schöllhorn, R. *Angew. Chem., Int. Ed. Engl.* **1988**, *27*, 1392.
(21) Grenier, J.-C.; Arrouy, F.; Locquet, J.-P.; Monroux, C.; Pouchard, M.; Villesuzanne, A.; Wattiaux, A. In *Phase Separation in Cuprate Superconductors*; Sigmund, E., Müller, K. A., Eds.; Springer-Verlag: Berlin, 1994.
(22) Goodenough, J. B.; Manthiram, A.; Paranthaman, P.; Zhen, Y. S. *Solid State Ionics* **1992**, *52*, 105.
(23) Goodenough, J. B.; Zhou, J. S.; Allan, K. *J. Mater. Chem.* **1991**, *1*, 715.
(24) Goodenough, J. B. *Pure Appl. Chem.* **1995**, *67*, 931.
(25) Goodenough, J. B. *Solid State Ionics* **1997**, *94*, 17.
(26) Manthiram, A.; Kuo, J. F.; Goodenough, J. B. *Solid State Ionics* **1993**, *62*, 225.
(27) Boldyrev, V. V. *Russ. Chem. Rev.* **1973**, *42*, 1161.
(28) Andersson, J. S. In *Proc. of the 7th International Symposium on the Reactivity of Solids*; Chapman and Hall: London, 1971.

to represent low-energy channels for oxygen diffusion. As one can see from dark field images, stacking faults are distributed inside the matrix with a periodicity of 30−100 Å. The penetration of the oxygen ions at the beginning of the process may proceed along these extended defects with a diffusion coefficient that is considerably higher as compared to the matrix values. At the same time individual domains can react with the oxygen ions coming from domain walls with a rate limited by a normal low diffusion coefficient for oxygen ions in metal oxides at room temperature ($D < 10^{-15}$ cm^2/s) but a rather short diffusion pathway (the size of domains is about tens of angstroms according electron microscopy data) which may drastically decrease the reaction time. A similar approach has been successfully applied earlier for the description of the mechanism of some topochemical reactions.[29,30]

We assume that the nature of extended defects and their formation mechanism is quite important for the understanding of the high reactivity of the $SrFeO_{2.5}$ at ambient temperature. It is obvious that further electron microscopy studies are required to identify the exact nature of these defects and to evaluate their concentration.

Acknowledgment. This work has been supported by Volkswagen-Stiftung. The authors are grateful to Dr. B. Bokhonov and Dr. A. Kolyshev for obtaining and indexing electron diffraction patterns.

CM980090V

(29) Goldberg, E.; Kovalenko, Yu. *Solid State Ionics* **1990**, *42*, 153.
(30) Lyakhov, N. In *Reactivity of Solids: Past, Present and Future*; Boldyrev, V. V., Ed.; Blackwell Science: Oxford, U.K., 1996.